



Computation of structural, electronic and optical properties of hybrid perovskite $CH_3CH_2NH_3GeBr_3$

¹Digpratap Singh, ²Anuradha Baghel

¹ Associate Professor, ² Research Scholar

¹ Department of Physics,

¹ Narain College, Shikohabad, Affiliated to Dr. B. R. Ambedkar University, Agra, India

Abstract: As the requirement of renewable energy is increasing, the efficiency of solar cell is needed to be increased. Hybrid perovskites are the materials that can be used to enhance the efficiency of solar cells due to their high power conversion efficiency. The researchers have found the properties of some lead-based hybrid perovskites to be optimal for a PV material. Since lead is toxic, researchers are trying to find its alternatives. In this work, Ethyl-ammonium germanium bromide ($CH_3CH_2NH_3GeBr_3$) is studied and its structural, electronic, and optical properties are obtained using FP-LAPW method implemented in the Wien2k code. The material absorption coefficient is found to be greater than the required minimum $10^4 cm^{-1}$ and bandgap is a direct band gap of 1.02 eV. The observed material has another advantage that it is lead (Pb) free. Thus, it is an eco-friendly and non-toxic material.

IndexTerms – Hybrid Perovskites, Solar Energy, Absorption Coefficient, Band Gap.

I. INTRODUCTION

Solar energy is an infinite energy source. However, it depends upon us that how efficiently we can utilize solar energy. Photovoltaic (PV) devices are used to convert solar energy into electrical energy. A good PV absorber should have greater absorption coefficient, appropriate band gap in visible range, high solar to electrical conversion efficiency and high charge carrier mobility. [1] Along with these, these should be able to remain stable at high temperature [2]. Recently, researchers have started exploring lead-based hybrid perovskite materials [3,4]. The general formula of these is $APbX_3$. Here, A is cation $CH_3NH_3^+$ and X^- is a halide anion. Although these hybrid perovskites have high conversion efficiency and cost is also low, still these are not commercially produced on a large scale since the toxic lead is present [5-10]. Hence, the exploration of lead-free hybrid perovskites is needed. Researchers have started working on this area. In this work, $CH_3CH_2NH_3GeBr_3$ is taken into study. It is lead-free material and thus will not be having environmental negative effects. It is checked whether it has the required properties of the potential PV material or not. The obtained results show that the material is suitable for PV material. The description of the material and obtained results are provided in the next sections.

The organization of the paper is as follows. Section 2 shows the used computational scheme. Section 3 presents the structural, electronic, and optical properties of the considered material. Section 4 concludes the paper.

II. COMPUTATIONAL DETAILS

Kohn-Sham equations [11] are solved to perform first principle calculations by the full potential linearized augmented plane wave method (FP-LAPW) as a theoretical account of DFT. WIEN2k [12-14] is used in this study. Authors in [15,16] have shown the accuracy of DFT to obtain the physical properties of the materials. In this study, $R_{mt} * K_{max}$ is taken as 3. K-mesh is of $8 \times 8 \times 8$ and 700 k-points are taken in the Full Brillouin Zone (FBZ). The Muffin tin radii of H, N, C, Br and Ge are taken as 0.6, 0.97, 0.95, 2.35 and 2.35 a.u. respectively. To avoid the charge leakage, core energy separation of -6 Ry is taken between valence and core electron. G_{max} is taken as 20. The charge and total energy convergence achieve the values of 0.001e and 0.0001 Ry. The density functional theory is taken into account since it provides accurate values for materials' physical properties [15,16].

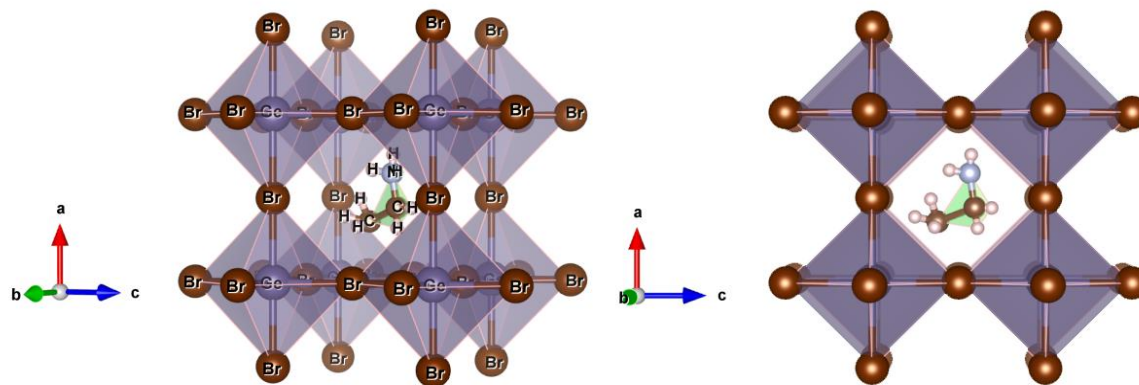


Figure 1: Crystal Structure of $CH_3CH_2NH_3GeBr_3$. Atom symbols are written in the left image. C,H and N atoms are at the center, Ge cation is in the octahedron and Br anion is at the corner of the octahedron.

III. RESULTS AND DISCUSSION

3.1 Structural Properties

Figure 1 shows the geometry of $CH_3CH_2NH_3GeBr_3$ in cubic phase. The two cations $CH_3CH_2NH_3^+$ and Ge^{2+} are forming bonds with Br^- . The Ge^{2+} cation is in the 6-fold coordination and it is then surrounded by GeI_6 octahedron. The cation $CH_3CH_2NH_3^+$ is in the interstitial site in the middle of the octahedron. Using the equation of state by Murnaghan [17], the volume optimization is done. Total energy is minimized by varying unit cell volume. It is shown in figure 2. Unit cell volume is found to be 1751.487 a.u.^3 , bulk modulus $B = 32.341 \text{ GPa}$ and pressure derivative $B' = 4.1665$

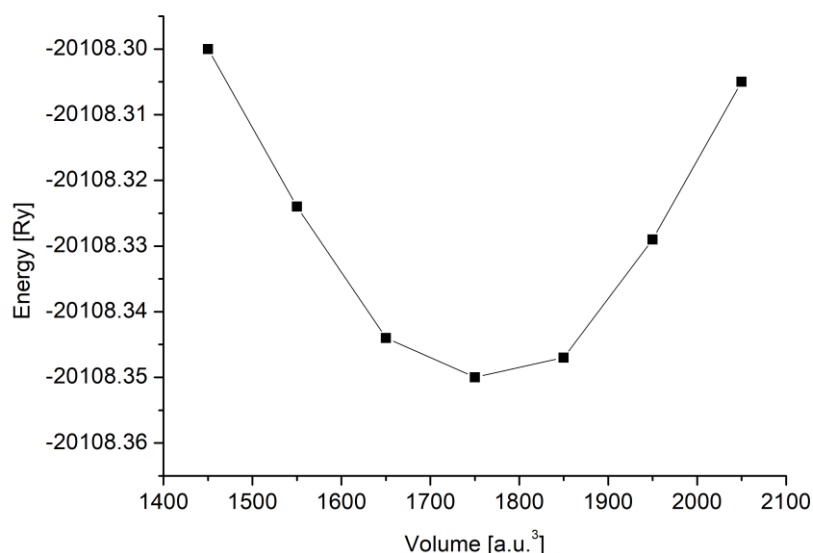


Figure 2: Energy vs volume for $CH_3CH_2NH_3GeBr_3$

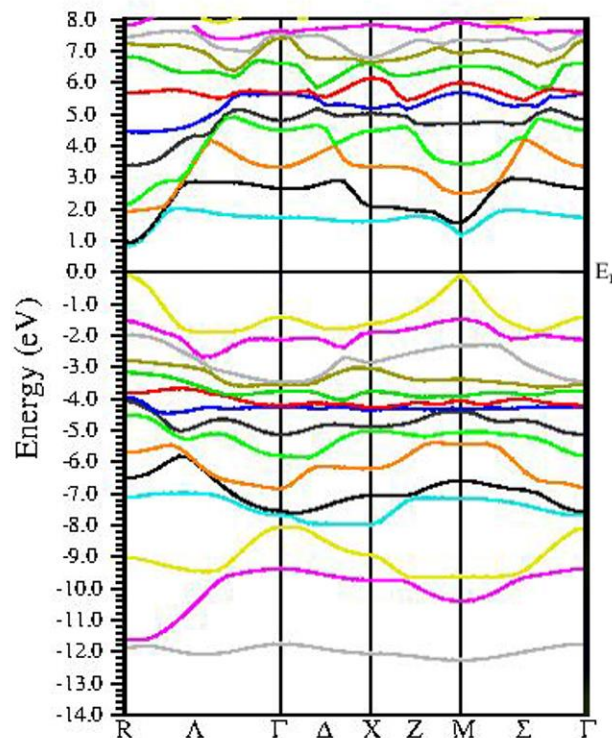


Figure 3: Band Structure of $\text{CH}_3\text{CH}_2\text{NH}_3\text{GeBr}_3$ hybrid perovskite with exchange correlation potential PBE.

3.2 Electronic Properties

Electronic properties (Density of states and band structure) are obtained by applying PBE exchange-correlation potential [18]. Density of states and band structure depends upon Ge-Br bonds, Br-Ge-Br bond angle and the size of $\text{CH}_3\text{CH}_2\text{NH}_3^+$ cation. The obtained band structure is shown in figure 3. Observing the plot at symmetry point R, it can be inferred that it is direct band gap material. Obtained band gap using PBE is 1.02 eV. This is the required range of bandgap to get high efficiency [19,20]. The band gap is attributed to the valence band (VB) and conduction band (CB) formed by the Ge-4s, Ge-4p and Br-4p orbitals. The study of partial density of states (PDOS) of C, N, Br and Ge along with the Total Density of States (TDOS) with PBE. All the PDOS and TDOS figures are combined into a single figure and shown in figure 4. We can infer the semiconducting property from the figure. conduction band is starting at around 1.02 eV and after that it is continuous. It is due to the Ge-4p and Br-4p states.

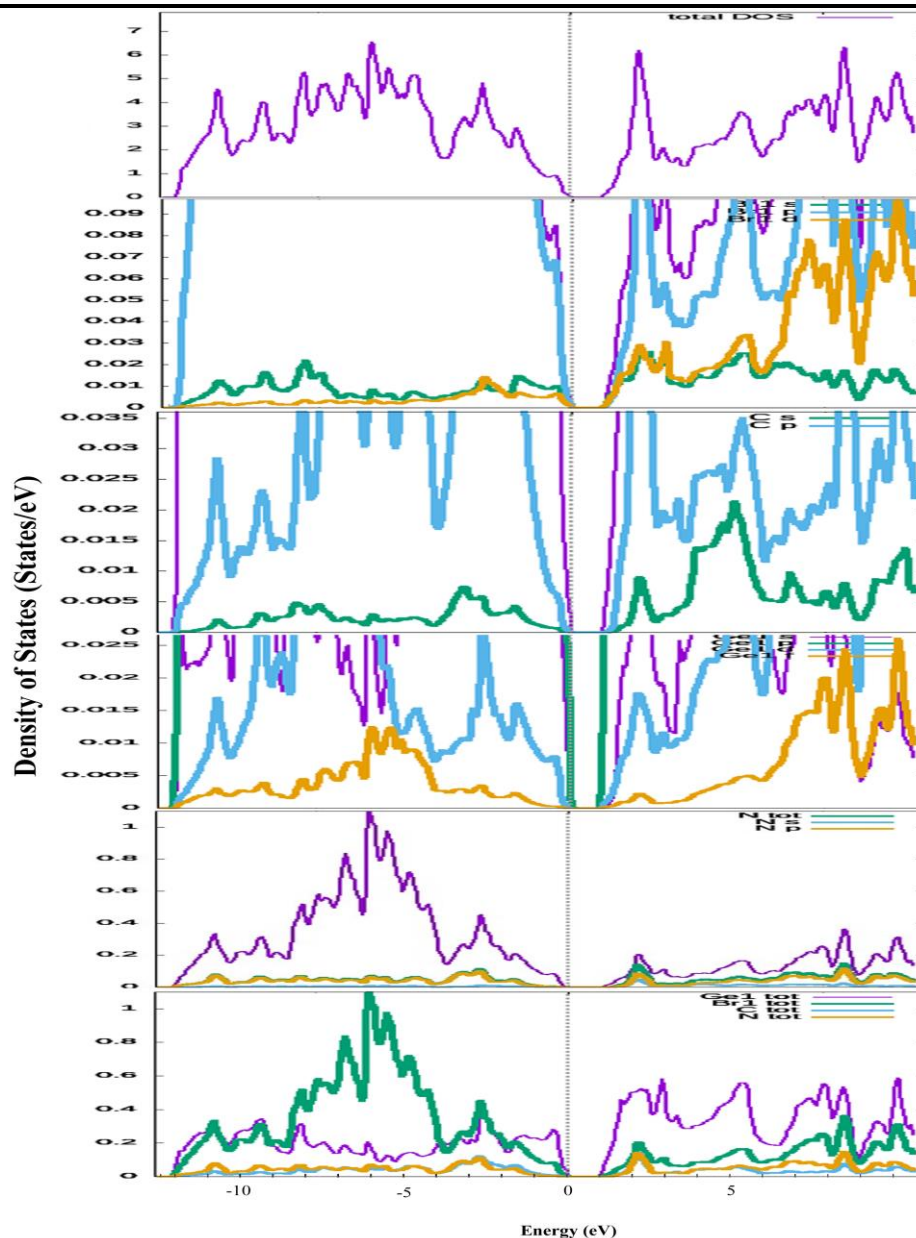


Figure 4: Total Density of States and Partial Density of States

3.3 Optical Properties

For the calculation of optical properties, electronic loss energy function, optical conductivity ($\sigma(\omega)$), and optical absorption ($\alpha(\omega)$) are calculated. These are calculated in terms of photon frequency ω dependent dielectric function $\epsilon(\omega)$. This is defined in [21,22]. In the simulation, an electron is considered in VB state and a photon having ω frequency is incident upon it. The electron is excited to the CB state by this photon. The $\epsilon(\omega)$ is calculated using equation 1.

$$\epsilon(\omega) = \epsilon_1(\omega) \pm i\epsilon_2(\omega) \dots \dots \dots (1)$$

$$\epsilon_2(\omega) = \frac{e^2 \hbar^2}{\pi^2 \omega^2} \sum_{v,c} |\psi_c | \hat{e}_j \cdot \vec{P} | \psi_v |^2 \delta(E_c - E_v - \hbar\omega) \dots \dots \dots (2)$$

In these equations, ψ_v is the VB state of energy eigenvalue E_v . ψ_c is the CB state of energy eigenvalue E_c . $|\psi_c | \hat{e}_j \cdot \vec{P} | \psi_v |$ are the momentum matrix elements between ψ_v and ψ_c . \hat{e}_j is the momentum operator. The optical properties can be inferred from $\epsilon_1(\omega)$ and $\epsilon_2(\omega)$. These are shown in subfigures (d) and (e) of figure 5. $\epsilon_1(\omega)$ shows the two peaks. of 12.2 and 3.9 at photon energy of 1.35 eV and 5.5 respectively. $\epsilon_1(\omega)$ is negative for all photon energy values greater than 8.9 eV. The electronic part of $\epsilon(0)$ is 10.5. It is called the static dielectric coefficient. This is an important parameter used in study of materials. $\epsilon_2(\omega)$ presents the energy absorption in the material. Three peaks are obtained in the figure 5(e). These peaks are related to direct inter-band transitions. $\alpha(\omega)$ is another parameter that is needed to select the PV material. It is called the absorption coefficient. It shows the absorbed energy as a fraction of incident energy per unit length. It is shown in figure 5(a). It starts increasing from 0 and exhibits the peaks on 2.7 eV, 6 eV and 8.25eV. It achieves highest value of $9.25 \times 10^5 \text{ cm}^{-1}$. These are the properties of semiconductors. The higher value of $\alpha(\omega)$ greater than 10^4 cm^{-1} is required for a PV material. Further, real part of optical conductivity ($\sigma(\omega)$) is shown in figure 5 (b). It has the highest value of $5.25 \times 10^3 \omega^{-1} \text{ cm}^{-1}$ for 8.25 eV incident photon energy. Energy lost by fast moving electron is calculated by energy

loss function. It is shown in figure 5 (c). It shows a peak of 0.18 at 4 eV. A constant magnitude of around 0.25 is shown in the range of photon energy 10-12 eV.

$$\epsilon_1(\omega) = \frac{2}{\pi} P \int_0^{\infty} \frac{\omega' \epsilon_2(\omega')}{\omega'^2 - \omega^2} d\omega' \quad \dots\dots\dots(3)$$

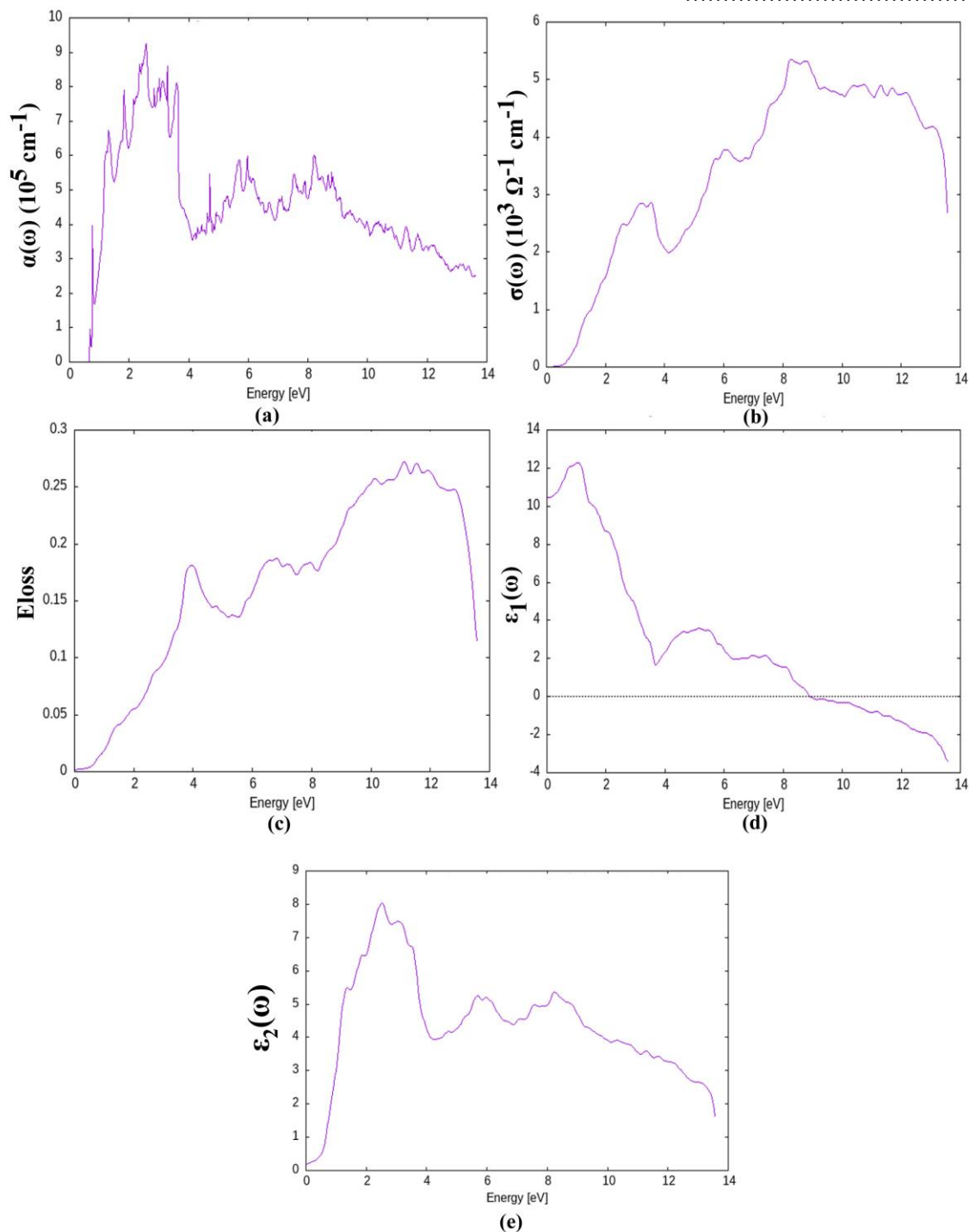


Figure 5: Optical Properties

IV. CONCLUSION

A potential photovoltaic material Ethyl-ammonium germanium bromide ($CH_3CH_2NH_3GeBr_3$) is studied in this work. Its structural, electronic, and optical properties were analyzed using FP-LAPW based on DFT with PBE using WIEN2k code. The material is found out a direct band gap material with a band gap 1.02 eV. The static dielectric constant is 10.5 and the absorption coefficient is higher than the required $10^4 cm^{-1}$. Thus the material is suitable for PV applications. The unit cell volume obtained after optimization is $1751.487 a.u.^3$, bulk modulus $B = 4.1665$ GPa, and pressure derivative B' is 4.1665 .

REFERENCES

- [1] Y. Zhao, H. Tan, H. Yuan, Z. Yang, J.Z. Fan, J. Kim, O. Voznyy, X. Gong, L.N. Quan, C.S. Tan, J. Hofkens, D. Yu, Q. Zhao, E.H. Sargent, Perovskite seeding growth of formamidinium lead iodide based perovskites for efficient and stable solar cells, Nat. Commun. 9 (2018) 1607.
- [2] P. Gao, M. Grätzel, M.K. Nazeeruddin, Organohalide lead perovskites for photovoltaic applications, Energy Environ. Sci. 7 (2014) 2448–2463.

- [3] B.Wook Park, S.I. Seok, Intrinsic instability of inorganic-organic hybrid halide perovskite materials, *Adv. Mater.* 31 (2019) 1805337.
- [4] K. Wang, D. Yang, C. Wu, M. Sanghadasa, S. Priya, Recent progress in fundamental understanding of halide perovskite semiconductors, *Prog. Mater. Sci.* 106 (2019) 100580.
- [5] W. Ke, M.G. Kanatzidis, Prospects for low-toxicity lead-free perovskite solar cells, *Nat. Commun.* 10 (2019) 965.
- [6] A. Krishna, S. Gottis, M.K. Nazeeruddin, F. Sauvage, Mixed dimensional 2d/3d hybrid perovskite absorbers: the future of perovskite solar cells?, *Adv. Funct. Mater.* 29 (2018) 1806482.
- [7] J. Chaudhary, S. Choudhary, C.M.S. Negi, S.K. Gupta, A.S. Verma, Surface morphological, optical and electrical characterization of methylammonium lead bromide perovskite ($\text{CH}_3\text{NH}_3\text{PbBr}_3$) thin film, *Phys. Scripta* 94 (2019) 105821.
- [8] C. Motta, F. El-Mellouhi, S. Sanvito, Charge carrier mobility in hybrid halide perovskites, *Sci. Rep.* 5 (2015) 12746.
- [9] C. He, G. Zha, C. Deng, Y. An, R. Mao, Y. Liu, Y. Lu, Z. Chen, Refractive index dispersion of organic-inorganic hybrid halide perovskite $\text{CH}_3\text{NH}_3\text{PbX}_3$ ($\text{X} = \frac{1}{4}\text{Cl}$, Br, I) single crystals, *Cryst. Res. Technol.* 54 (2019) 1900011.
- [10] Z. Zhang, D. Liu, K. Wu, First-principles study of structural stability, electronic and optical properties of GAdoped MAPbI_3 , *Spectrochim. Acta Mol. Biomol. Spectrosc.* 226 (2020) 117638.
- [11] P. Hohenberg, W. Kohn, Inhomogeneous electron gas, *Phys. Rev.* 136 (1964) B864–B871.
- [12] W. Kohn, L.J. Sham, Self-consistent equations including exchange and correlation effects, *Phys. Rev.* 140 (1965) A1133–A1138.
- [13] P. Blaha, K. Schwarz, G.K.H. Madsen, D. Kvasnicka, J. Luitz, R. Laskowski, F. Tran, L.D. Marks, WIEN2k, an Augmented Plane Wave plus Local Orbitals Program for Calculating Crystal Properties, Karlheinz Schwarz, Techn Universität Wien, Austria, 2018, ISBN 3-9501031-1-2.
- [14] P. Blaha, K. Schwarz, P. Sorantin, S. Trickey, Full-potential, linearized augmented plane wave programs for crystalline systems, *Comput. Phys. Commun.* 59 (1990) 399–415.
- [15] R. Muhammad, Y. Shuai, H. Tan, H. Muhammad, Theoretical perspective on structural, electronic and magnetic properties of 3d metal tetraoxide clusters embedded into single and di-vacancy graphene, *Appl. Surf. Sci.* 408 (2017) 21–33.
- [16] R. Muhammad, Y. Shuai, H. Tan, A first-principles study on alkaline earth metal atom substituted monolayer boron nitride (BN), *J. Mater. Chem. C* 5 (2017) 8112–8127.
- [17] F.D. Murnaghan, On the theory of the tension of an elastic cylinder, *Proc. Natl. Acad. Sci. Unit. States Am.* 30 (1944) 382–384.
- [18] J.P. Perdew, K. Burke, M. Ernzerhof, Generalized gradient approximation made simple, *Phys. Rev. Lett.* 77 (1996) 3865–3868.
- [19] W.E.I. Sha, X. Ren, L. Chen, W.C.H. Choy, The efficiency limit of $\text{CH}_3\text{NH}_3\text{PbI}_3$ perovskite solar cells, *Appl. Phys. Lett.* 106 (2015) 221104.
- [20] W. Shockley, H.J. Queisser, Detailed balance limit of efficiency of p-n junction solar cells, *J. Appl. Phys.* 32 (1961) 510–519.
- [21] M.Q. Cai, Z. Yin, M.S. Zhang, First-principles study of optical properties of barium titanate, *Appl. Phys. Lett.* 83 (2003) 2805–2807.
- [22] R. Muhammad, M.A. Unar, I. Ahmed, A.R. Chachar, Y. Shuai, Ab-initio investigations on physisorption of alkaline earth metal atoms on monolayer hexagonal boron nitride (h-BN), *J. Phys. Chem. Solid.* 118 (2018) 114–125.